

Research Article

DOI: <http://dx.doi.org/10.22192/ijamr.2022.09.02.003>

## Synthesis, spectral, NLO and DFT studies on 6-methylbenzotriazolium picrate crystal

S. Sasikala<sup>1</sup>, P. Anbusrinivasan<sup>2</sup>, T. Dhanabal<sup>3\*</sup>, B. Raja<sup>3</sup>

<sup>1</sup>Department of Chemistry, Vivekananda College of Arts and Science for Women, Sirkali, Tamil Nadu, India.

<sup>2</sup>Department of Chemistry, A.V.C College (Autonomous), Mannampandal, Mayiladuthurai, Tamil Nadu, India.

<sup>3</sup> Department of Chemistry, Muthayammal College of Engineering, Rasipuram, Namakkal-637408, Tamil Nadu, India.

\*Corresponding author: Email Address: [dhanabal27@gmail.com](mailto:dhanabal27@gmail.com)

### Abstract

#### Keywords

Crystallization,  
X-ray diffraction,  
Thermal analysis,  
FTIR spectrum,  
SHG efficiency,  
DFT study.

6-methyl benzotriazolium picrate, a new single crystal has been grown from respective aqueous solutions by using slow evaporation method at room temperature. The crystallinity of the crystal was ascertained by powder X-ray diffraction pattern method. The UV-visible absorption study was studied to ascertain the optical property of the crystal. The thermal stability and decomposition pattern of the crystal were formulated using TG-DTA analyses. The functional groups present in the crystal were determined by FTIR spectral study. The Kurtz-Perry powder technique was used to find out the SHG efficiency of the title crystal. The dielectric constant and loss of the crystals were studied and shows that the both decrease with increases in frequency. The HOMO-LUMO energy gap reveals the intra-molecular charge transfer interaction occurs within the molecule studied by DFT calculation study.

### 1. Introduction

Nonlinear optical crystals have been a great deal of attention in topical years due to their potential use in the fields like laser technology, optical communication, optical data storage and optical signal processing [1-3]. It is also contributing numeral of applications in the domain of optoelectronics and photonic technologies [4,5].

The NLO materials in their single crystal form exhibiting large optical nonlinearity are also of giant interest for telecommunication, optical information processing, and high optical disk data storage [6-8]. Hence, there is a great demand to synthesize new NLO materials and grow their single crystals. Over recent years a series of studies have been performed on organic optical materials with high nonlinearity for variety of

applications in electro-optic and second harmonic generation (SHG) devices [9-12]. The origin of nonlinearity in these materials is due to the presence of delocalized Pi-electron systems connecting donor and acceptor groups, which enhance their asymmetric polarizability [13]. Many new organic crystals have been examined based on the predictive molecular engineering approach and have been shown to have potential applications [14]. Other advantages of organic compounds involve amenability for synthesis, multifunctional substitution, higher resistance to optical damage and maneuverability for device application etc. [15]. The various organic sub-networks induce noncentrosymmetry in the bulk and enhance the thermal and mechanical stabilities through hydrogen bonding interactions [16, 17]. Organic crystals are increasingly being renowned as materials of the potential since of their molecular nature combined with the adaptability of synthetic chemistry can be used to modify and optimize their molecular structure in order to maximize nonlinear properties [18]. Picric acid forms crystalline picrate salts with various organic molecules by virtue of its acidic nature and forms salts through explicit electrostatic or hydrogen bonding interactions [19]. The strength and nature of the electron donor-acceptor type bonding in the picric acid crystal are dictated by the nature of the partners implicated in the bond formation process [20]. The linkage encompasses electrostatic interactions as well as the intermolecular interaction between picric acid and partner such as hydrogen bonding [21]. Bonding of picric acid as a proton donor strongly depends on the relationship of its acidity (pKa) with the basicity (pKb) of the partner. Organic materials are in

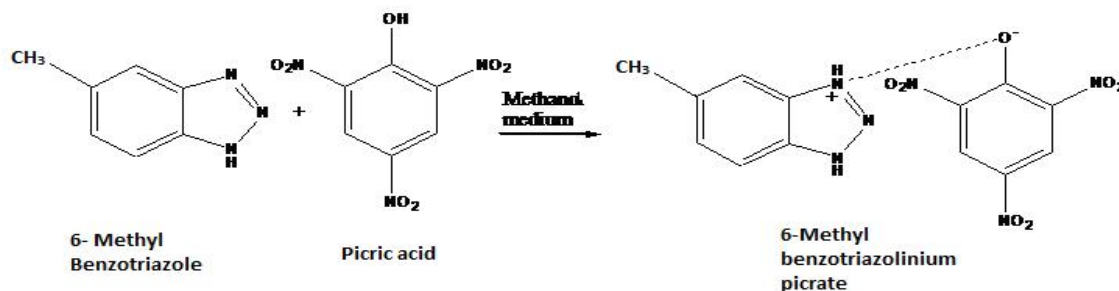
increasing demand, as they are superior candidates for nonlinear optical and electro-optic device applications than those of inorganic materials. In adding together, picric acid is also used at human therapy like treatment of burns, antiseptic and astringent agent [22].

In the present exploration, the growth aspects of 6-MBTP have been studied and the grown crystal has been characterized by various preliminary techniques such as Single crystal X-ray diffraction, Powder X-ray diffraction, UV-visible absorption, FTIR, TG-DTA, NLO, dielectric and DFT studies have been studied.

## 2. Experimental details

### 2.1. Synthesis of 6-methyl benzotriazolium picrate single crystals.

Single crystals of 6-methylbenzotriazolium picrate were synthesized by slow evaporation solution growth method. Methanolic solution of picric acid was added to methanolic solution of 6-methylbenzotriazole in 1:1 molar ratio. The two solutions were mixed together and stirred well for about 6 h to get a homogeneous solution using mechanical stirrer and the resultant solution was filtered into a clean dry beaker through a Whatman 40 filter paper. After filtration, the beaker was covered by an ordinary filter paper. The filtrate was then allowed to crystallize in dust-free environment at ambient temperature. Care was taken to minimize the temperature variation and mechanical disturbance during crystal growth. The synthetic procedure of 6-MBTP crystal is given in scheme 1.



**Scheme 1.** Synthetic reaction of 6-MBTP crystal

Within 15 to 25 days, bright, transparent and yellow coloured 6-MBTP crystals were obtained with average dimension of  $0.5 \times 0.3 \times 0.2 \text{ cm}^3$ . The grown crystals were collected from the mother liquid by using well cleaned forceps. The harvested crystals were recrystallized repeatedly to get a good quality of the crystals.

## 2.2. Physico-chemical characterization of 6-MBTP crystal

The single crystal X-ray diffraction data of the crystal was collected at 298 K on a Bruker SMART APEX CCD, area detector system [  $(\text{Mo K } \alpha) = 0.7103 \text{ \AA}$ ]. The powder XRD patterns of BTCC crystal were obtained using BRUKER AXS D8 Advance X-ray diffractometer model instrument with Cu K radiation ( $\lambda = 1.54060 \text{ \AA}$ ) at room temperature. The UV-VIS-NIR absorption study of the crystal was carried out using JASBO V-550 spectrometer. The TG-DTA of the crystal was recorded using a PERKIN ELMER DIAMOND thermal analyzer under nitrogen. The FTIR spectrum of the crystal was recorded using a Perkin Elmer model RX1 instrument. The SHG efficiency of the crystal was carried out by modified Kurtz-Perry powder

technique using Nd:YAG laser. The dielectric properties of the crystal were studied at room temperature using a TH 2816 A DIGITAL LCRZ METER in the frequency region from 50 Hz to 5 MHz. The DFT study of the crystal was also studied by quantum chemical descriptors.

## 3. Result and Discussion

### 3.1. Single crystal X-ray diffraction study

From the unit cell parameters data the synthesized crystal belongs to orthorhombic system. The unit cell dimensions are  $a = 19.6453 \text{ \AA}$ ,  $b = 8.5439 \text{ \AA}$ ,  $c = 4.1946 \text{ \AA}$ , volume =  $704.06 (\text{ \AA})^3$  and  $\alpha = \beta = \gamma = 90^\circ$  and with space group  $P212121$ . This space group is recognized as noncentro symmetric, thus satisfying the basic and essential material requirement for the SHG activity of the crystal. It has been observed that  $P212121$  is one among the most popular space group and it allows maximal contribution of the molecular nonlinearity of the macroscopic crystal nonlinearity. The unit cell parameters data the synthesized crystal is given in Table 1.

**Table 1.** Single crystal X-ray diffraction data of 6-MBTP crystal.

Unit cell Parameters	Values
a	19.6453
b	8.5439
c	4.1946
	$90^\circ$
	$90^\circ$
	$90^\circ$
Volume	$704.06 (\text{ \AA})^3$
Crystal System	Orthorhombic

### 3.2. Powder X-ray diffraction pattern study

The powder X-ray diffraction pattern of 6-MBTP crystal is shown in Figure 1. The powder X-ray diffraction data of 6-MBTP crystal is given in Table 2. The sharp and well defined Bragg peaks at  $2\theta$  angle indicates the crystalline of the crystal.

The sharp and well defined Bragg peaks observed in the powder and simulated X-ray diffraction patterns confirm its crystalline nature of the grown crystal. The cell parameters of the crystal indicate that the crystal belongs to orthorhombic system.

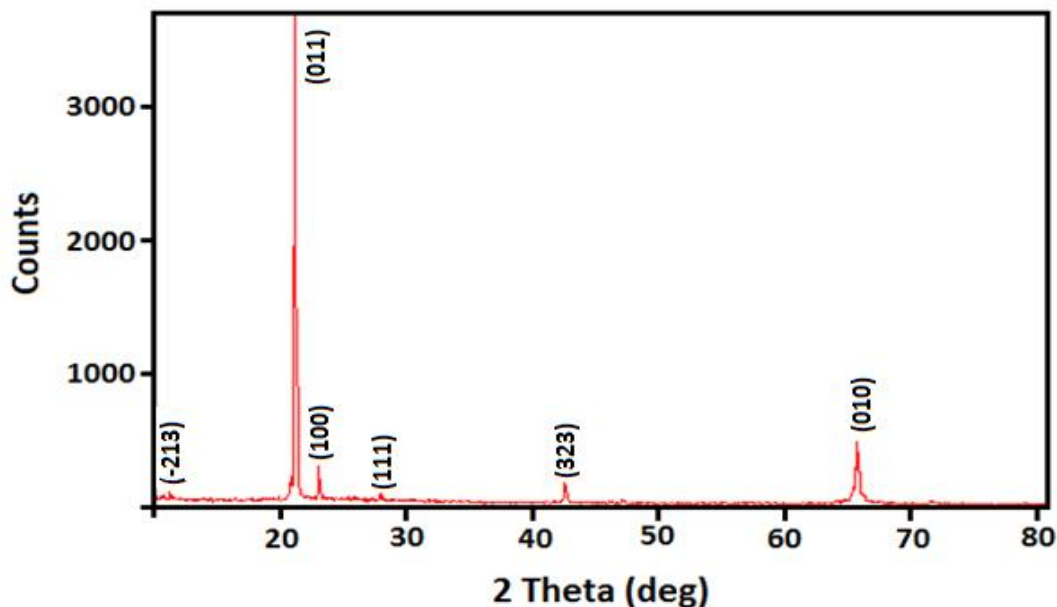


Figure 1. Powder X-ray diffraction pattern of the crystal.

**Table 2.** Powder X-ray diffraction data of 6-MBTP crystal.

h	k	l	d-Spacing (Obs) [Å <sup>0</sup> ]	d-Spacing (Cal) [Å <sup>0</sup> ]	2Th (Obs) [deg]	2Th (Cal) [deg]	Rel.Int. [%]	FWHM Left [ <sup>0</sup> 2 Th]
1	1	0	7.9024	7.8959	11.197	11.284	1.92	0.1476
0	2	0	4.2726	4.2692	20.790	20.776	3.30	0.1968
0	0	1	4.1985	4.1951	21.161	21.164	100.00	0.1476
2	0	1	3.8600	3.8576	23.037	23.037	7.61	0.1476
4	0	1	3.1906	3.1880	27.965	27.950	1.20	0.2952
8	0	1	2.1215	2.1197	42.618	42.629	3.43	0.2460
4	4	0	1.9597	1.9581	46.331	46.315	0.45	0.2952
4	0	2	1.9303	1.9288	47.077	47.077	0.95	0.1476
1	6	0	1.4215	1.4204	65.685	65.690	11.16	0.1968

### 3.3. UV-visible absorption spectral study

The absorption spectrum is very important for any single crystal which can be useful for any practical application, only if it has a wide transparency window. The UV-visible spectrum of 6-MBTP is shown in Figure 2. The absorption

peaks observed at 240 and 280 nm are due to electronic transitions. There is no absorption between 300 and 1200 nm. The  $\pi$ - $\pi^*$  transitions is assigned to charge transfer in the synthesized crystal. Hence it is very useful for opto-electronic applications.

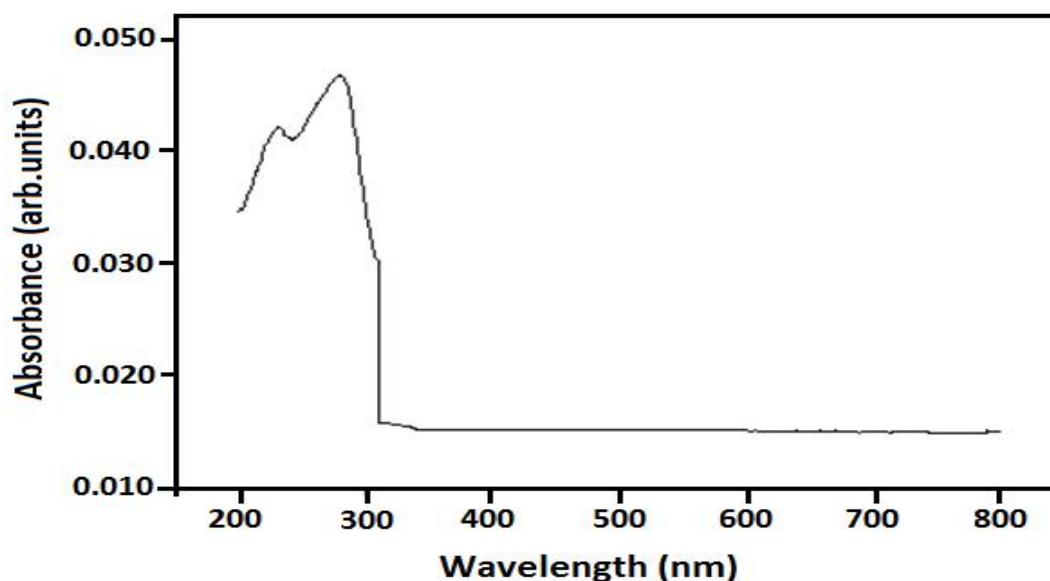


Figure 2. UV-visible absorption spectrum of the crystal.

### 3.4. Thermal analyses

#### 3.4.1. TG analysis

The TGA thermogram of the crystal is given in Figure 3. The thermal behavior of crystal is studied using TGA analysis. The crystal decomposes in a single stage when it is heated from room temperature up to 185°C. The crystal is stable up to 185°C afterwards it decomposes in a single

stage between 185°C and 305°C. The single stage weight loss due to removal of hydro-carbons. The experimental weight loss is 98%. Then the calculated weight loss is 100%. These differences are weight loss due to presence of occluded and absorbed water molecules.

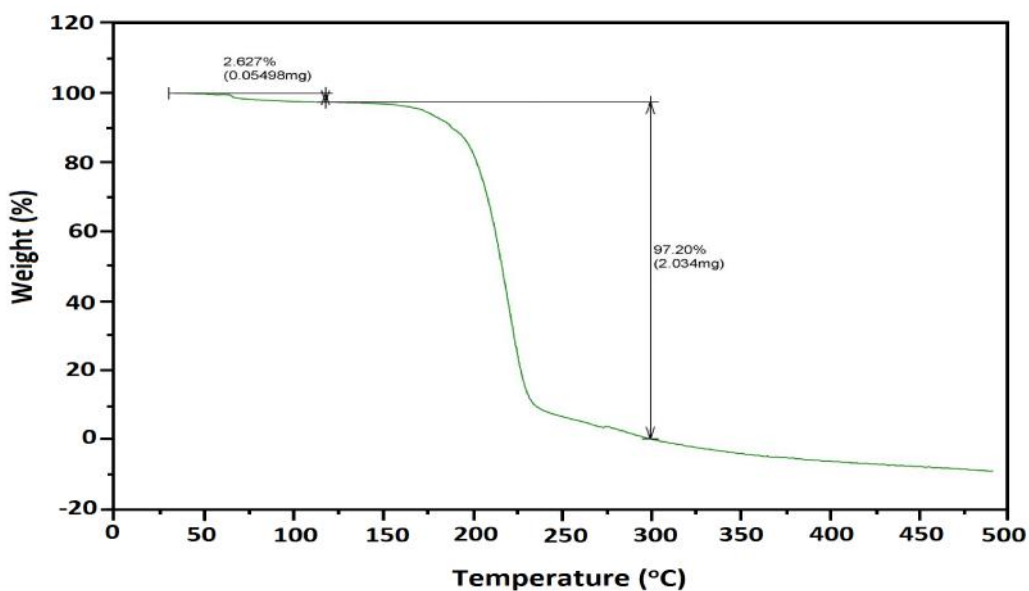


Figure 3. TGA thermogram curve of the crystal.

### 3.4.2. DTA study

The DTA thermogram of the crystal is shown in Figure 4. The Peak 108.20°C is due to the

occlusion of the water molecules. The sharp peak at 228.34°C is assigned to single stage decomposition of the crystal.

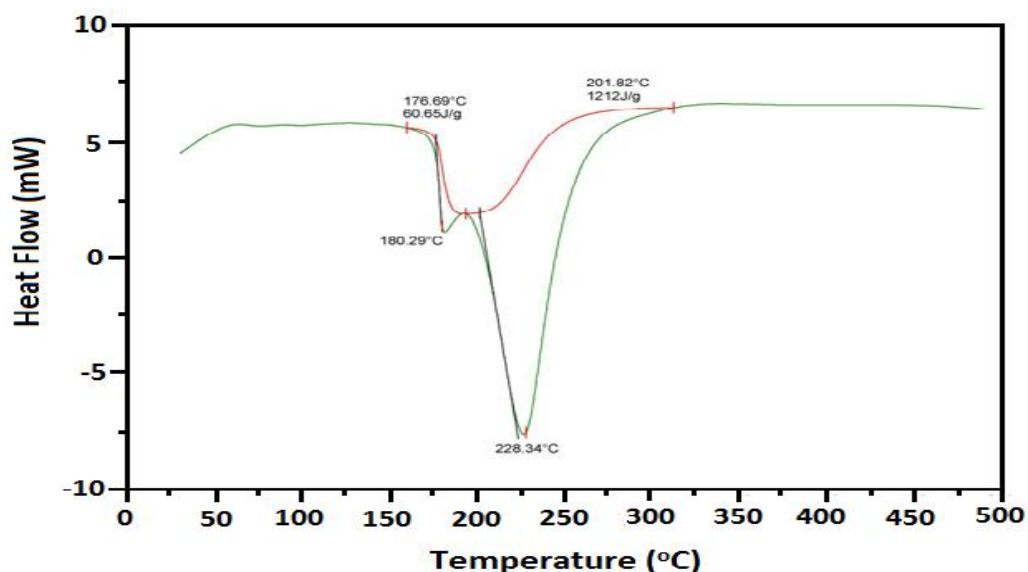


Figure 4. DTA thermogram of the crystal.

### 3.5. FTIR spectral analysis

The FTIR spectrum of 6-MBTP was carried out between 4000 and 400  $\text{cm}^{-1}$ . The observed spectrum is shown in Figure 5. The asymmetric stretching of NH molecule peak observed at 3798  $\text{cm}^{-1}$ . The peaks at 3394 and at 3298  $\text{cm}^{-1}$  are due to the NH stretching vibrational bands in NH. The  $\text{NH}_2$  group associated with broad band is

found at 3149  $\text{cm}^{-1}$ . The peak at 2688  $\text{cm}^{-1}$  is due to asymmetric stretching vibration  $\text{NH}^+$  molecule. The peak at 2342  $\text{cm}^{-1}$  is presence of NH stretching vibration. The stretching vibration of  $\text{CH}_2$  is observed at 2217  $\text{cm}^{-1}$ . The peak at 2035  $\text{cm}^{-1}$  is due combination band of  $\text{NH}^+$ .

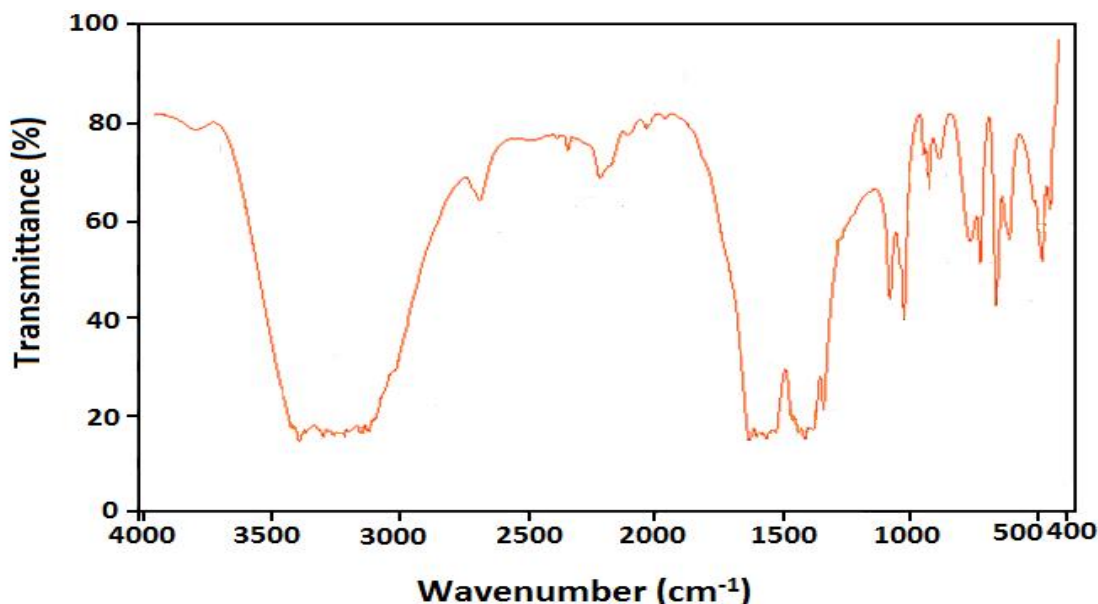


Figure 5. FTIR spectrum of the crystal.

The band observed at  $1567\text{ cm}^{-1}$  is presence of symmetric stretching of  $\text{NH}_2$ . The wagging of  $\text{CH}_2$  is found at  $1343\text{ cm}^{-1}$ . The peak at  $1416\text{ cm}^{-1}$  is due to C-NH stretching vibration. The peak at  $1028\text{ cm}^{-1}$  is due to -CN stretching vibration. The peak at  $892\text{ cm}^{-1}$  and  $933\text{ cm}^{-1}$  indicates the rocking

of  $\text{CH}_2$ . The symmetric N-C-N stretching vibration is found at  $667\text{ cm}^{-1}$ . The peak at  $617\text{ cm}^{-1}$  indicates that presence of symmetric C-N-C stretching mode. The O-N-O stretching vibration is found at  $488\text{ cm}^{-1}$ . The FTIR data of the crystal is given in Table 3.

**Table 3.** FTIR spectral data of 6-MBTP crystal.

Wavenumber( $\text{cm}^{-1}$ )	Assignment
3798	Asymmetric Stretching of NH molecule
3394	Stretching vibrational bands in NH
3298	
3149	NH group associated with broad band
2688	Asymmetric stretching vibration of $\text{NH}^+$ molecule
2342	NH Stretching vibration
2217	Stretching vibration of $\text{CH}_2$
2035	Combination band of $\text{NH}^+$
1343	Wagging of $\text{CH}_2$
1416	C-NH stretching vibration
1028	-CN stretching vibration
892	Rocking of $\text{CH}_2$
731	$\text{NO}_2$ and phenyl ring out-of-plane bending vibration
667	ONO stretching vibration
617	Symmetric N-C-N stretching
488	C-N-C stretching mode

### 3.6. Non-linear optical study

Kurtz-Perry test was examined to find the NLO property of the 6-MBTP crystal. Kurtz technique is used as a screening technique to identify the materials with the capacity for phase matching in addition to identifying the materials with non-Centrosymmetric crystal structures. The crystals were ground into powder and densely packed in between two glass slides. An Nd:YAG laser beam of pulse width 10 ns at a wavelength of 1064 nm and 10Hz fundamental radiation was made to fall normally on the sample cell. The proton donor picrate anion and proton acceptor imine group (-NH) in the complex provide infra structure to introduce the charge asymmetry formed. The SHG efficiency of the potassium dihydrogen

phosphate and the complex has been measured as 20 mV and 43 mV respectively. It is observed that the SHG efficiency of the grown 6-MBTP crystal was found to be twice than that of KDP.

In the structure of 6 methyl benzotriazolium picrate, the cations and anions are linked by strong intermolecular N-H...O and C-H...O hydrogen bonds. Intermolecular hydrogen bonding is formed between the hydrogen atoms of the protonated amino group in 6 methylbenzotriazolium cation and the negatively charged oxygen atom of the picrate ion in 6-benzotriazolium picrate crystal will enhance the hyperpolarizability value. This is one of the reasons for a crystal to exhibit SHG efficiency.

### 3.7. Dielectric studies

The dielectric measurement of 6-MBTP crystal was carried out using LCR meter in the frequency from 50 Hz to 5 MHz. The sample was polished by soft tissue paper. Silver paste was applied on both opposite faces to make a capacitor with the crystal as a dielectric medium. The sample was placed between two copper electrodes, which acts as a parallel plate capacitor. The capacitance and dielectric loss were measured for different frequencies from 50 Hz to 5 MHz. The dielectric constant was calculated using the following relation

$$\epsilon_r = Ct / \epsilon_0 A$$

where C is the capacitance, d is the thickness of the crystal,  $\epsilon_0$  is the vacuum dielectric constant and A is the area of the crystal.

The variation of dielectric constant with log frequency is given in Figure 6. The graph, it indicates that the dielectric constant of the crystal decreases with increase in frequency, which is due to effect

of charge distribution by mass carrier hopping on defects. The values of dielectric constants are high at lower frequencies and they are low at higher frequency region and the large values of dielectric constant at lower frequencies suggest that there is a contribution from all the four known sources of polarizations namely, electronic, ionic, dipolar and space charge polarizations. Space charge polarization is generally active at lower frequencies. The space charge polarization will depend on the purity and low perfection of the material.

The variation of dielectric loss with log frequency is shown in Figure 7. From the graph, it is observed that the dielectric loss decreases with increase in frequencies. The values of dielectric loss are high at lower frequencies and are low at higher frequency region. The low values of dielectric loss suggest that the sample possesses enhanced optical quality with lesser defects and this parameter is of vital importance for optoelectronic applications.

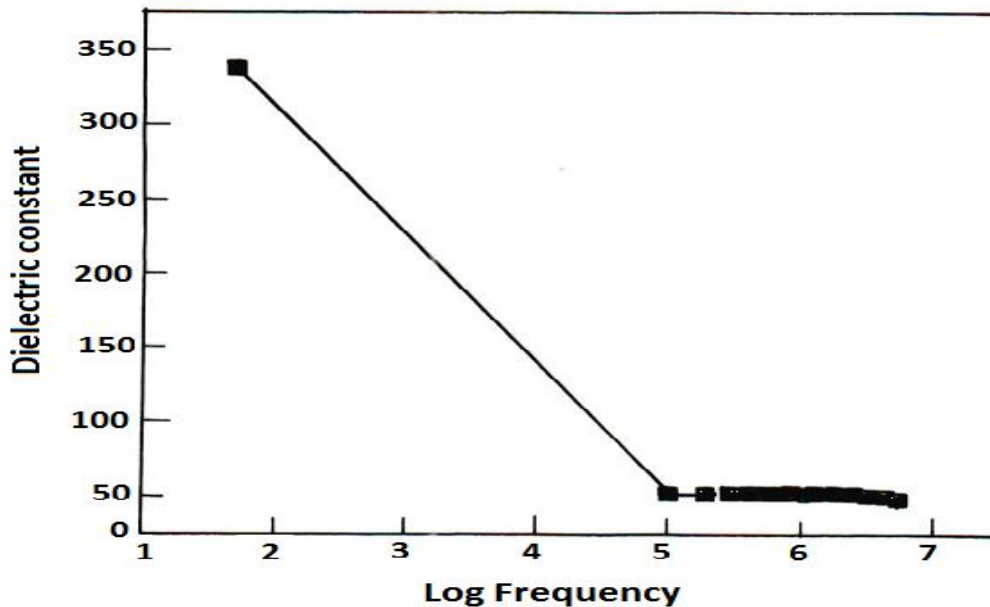


Figure 6. Variation of dielectric constant with log frequency



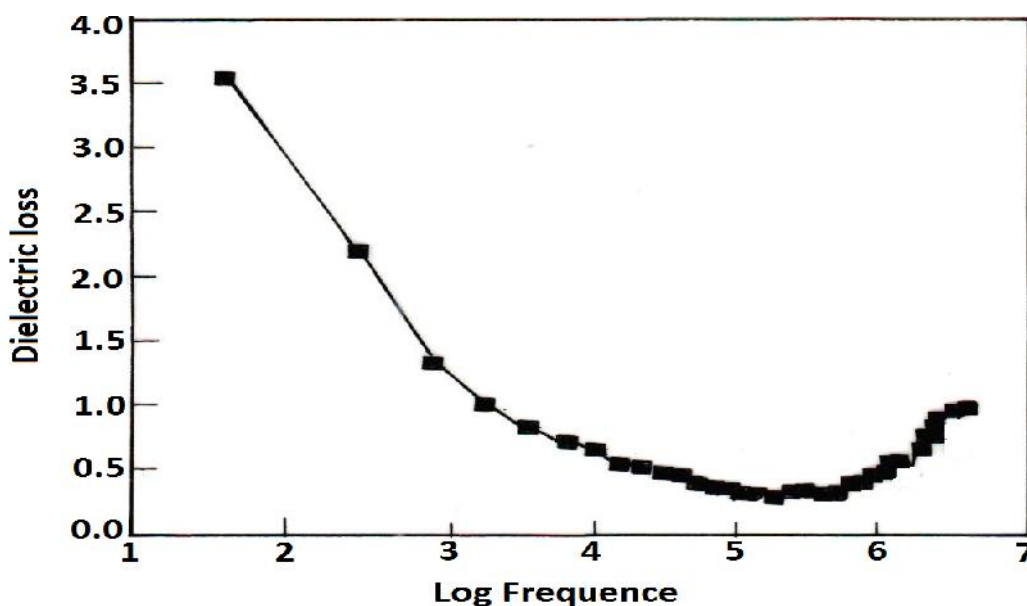


Figure 7. Variation of dielectric loss with log frequency

### 3.8. DFT study

Density Functional Theory (DFT) of chemical reactivity is known conceptual density functional theory. One of the aims of the conceptual density functional theory is to calculate the quantum chemical descriptors like hardness ( $\chi$ ), electronegativity ( $\mu$ ) and chemical potential ( $\mu$ ) giving useful hints about the stability of reactivity of chemical species. In this theory, aforementioned quantum chemical descriptors are calculated via following equations including ground state ionization energy and electron affinity values of chemical species (atoms, ions and molecules). Here it is important to note that electronegativity is described as the negative of chemical potential [23-26].

$$\chi = -\frac{I + A}{2} \quad (1)$$

$$\mu = \frac{I - A}{2} \quad (2)$$

Softness ( $\sigma$ ) that is a measure of the polarizability of chemical species is defined as the multiplicative inverse of chemical hardness ( $\sigma = 1/\chi$ ).

Electrophilicity ( $\omega$ ) and nucleophilicity are two useful chemical reactivity indices. Parr who made many studies on chemical reactivity proposed the following formula to calculate the electrophilicity index depending on electronegativity and hardness values of chemical species. In addition, he described the nucleophilicity ( $\nu$ ) as the multiplicative inverse of electrophilicity ( $\nu = 1/\omega$ ).

$$\omega = \frac{\chi^2}{2\eta} \quad (3)$$

$$\nu = \frac{E_{HOMO} + E_{LUMO}}{2} \quad (4)$$

$$\eta = \frac{E_{HOMO} - E_{LUMO}}{2} \quad (5)$$

The energies of the highest occupied molecular orbital (HOMO) and the lowest unoccupied molecular orbital (LUMO) are computed at various level. HOMO and LUMO orbitals for the crystal are shown Figure 8. The DFT data of the crystal is given in Table 4. Generally the energy values of LUMO, HOMO and their energy gap reflect the chemical activity of the molecule.

HOMO as an electron donor represents the ability to donate an electron, while LUMO as an electron acceptor represent the ability to receive an electron [27-29]. The HOMO and LUMO orbitals of the crystal are given in Figure 9 and 10 respectively. The energies of the HOMO [-8.612eV, -9.823eV, 11.183eV, -9.303eV] and

LUMO [2.748eV, 2.829eV, 2.884eV, 2.966eV] and the energy gaps are found to be -11.360eV - 12.653eV -14.067eV and -12.272eV. The molecular electron repulsion orbital of the crystal is given in Figure 11. The HOMO-LUMO energy gap reveals the intra-molecular charge transfer (ICT) interaction occurs within the molecule.

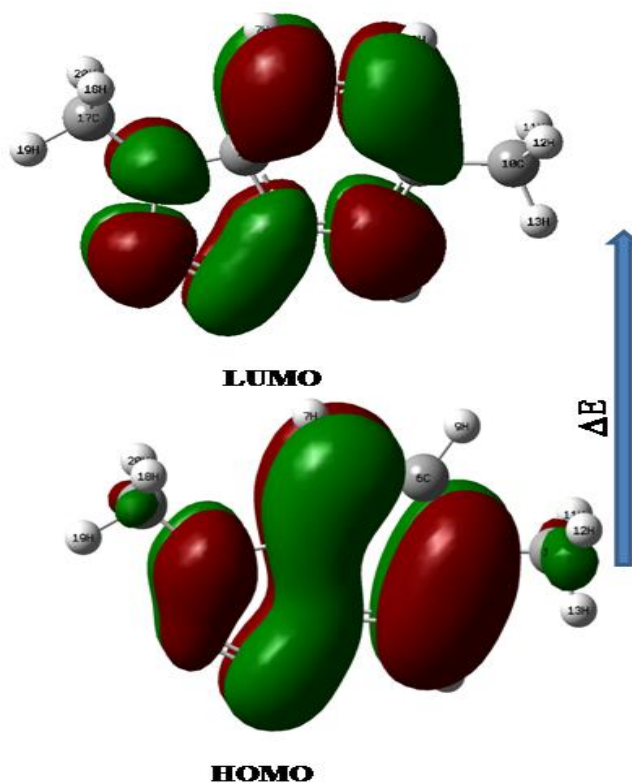


Figure 8. Energy gap of HOMO and LUMO orbitals of the crystal

Table 4 DFT data of the 6-MBTP crystal.

Methods	HOMO	IE	LUMO	EA	E		(eV)	(eV)		$\epsilon$	
B3LYP/321	-8.612	8.612	2.748	-2.748	-	11.360	2.932	5.680	0.176	0.756	1.321
B3LYP/6-311(d,p)	-9.823	9.823	2.829	-2.829	-	12.653	3.496	6.326	0.158	0.966	1.034
B3LYP/321	-11.183	11.183	2.884	-2.884	-	14.067	4.149	7.034	0.142	1.224	0.817
B3LYP/6-311(d,p)	-9.306	9.306	2.966	-2.966	-	12.272	3.170	6.136	0.163	0.818	1.221



The dielectric constant and dielectric loss of the crystals were decreases with increases in frequency. The DFT calculation study was studied to find out the HOMO–LUMO energy gap and intra-molecular charge transfer (ICT) interaction occurs within the molecule.


## Acknowledgments

The authors gratefully acknowledge the Secretary and Principal of Vivekananda College of Arts and Science for Women, Sirkali, Tamil Nadu, India, for their constant encouragement and support and also gratefully acknowledge A.V.C College (Autonomous), Mannampandal, Mayiladuthurai, Tamil Nadu, India, for their constant encouragement and support. The one of the author T.Dhanabal gratefully acknowledges the Chairman, Secretary of Muthayammal College of Engineering, Rasipuram, Namakkal-637408, Tamil Nadu, India for their constant encouragement and support.

## References

- [1] H.O. Marcy, L.F. Warren, M.S. Webb, C.A. Ebbbers, S.P. Velsko, G.C. Kennedy, G.C. Catella, *Appl. Opt.* 31 (1992) 5051.
- [2] D.S. Chemla, J. Zyss (Eds.), *Nonlinear Optical Properties of Organic Molecules and Crystals*, vols. I and II, Academic Press, New York, 1987.
- [3] H.O. Marcy, M.J. Rosker, L.F. Warren, P.H. Cunningham, C.A. Thomas, L.A. De Loach, S.P. Velsko, C.A. Ebbbers, J.-H. Liao, M.G. Kanatzidis, *Opt. Lett.* 20 (1995) 252.
- [4] X.Q. Wang, D. Xu, D.R. Yuan, Y.P. Tian, W.T. Yu, S.Y. Sun, Z.H. Yang, Q. Fang, M.K. Lu, Y.X. Yan, F.Q. Meng, S.Y. Guo, G.H. Zhang, M.H. Jiany, *Mater. Res. Bull.* 34 (1999) 2003.
- [5] X.L. Duan, D.R. Yuan, X.Q. Wang, X.F. Cheng, Z.H. Yang, S.Y. Guo, H.Q. Sun, D. Xu, M.K. Lu, *Cryst. Res. Technol.* 37 (2002) 446.
- [6] I. Ledoux, *Synth. Metal*, 54 (1993) 123.
- [7] D.R. Yuan, D. Xu, N. Zhang, M.G. Liu, M.H. Jiang, *Chin. Phys. Lett.* 13 (1996) 841.
- [8] M. Wai, T. Kobayashi, H. Furry, Y. Mori, T. Sasaki, *J. Appl. Phys. Jpn.* 36 (1997) 276.
- [9] J.D. Bierlin, L.K. Cheng, Y. Wang, W. Tam, *Appl. Phys. Lett.* 56 (1990) 423.
- [10] S.C. Sabarwal, N. Sangeetha, *J. Crystal Growth*, 187 (1998) 253.
- [11] R.N. Rai, P. Ramasamy, C.W. Lan, *J. Crystal Growth*, 253 (2002) 499.
- [12] A.M. Petrosyan, H.A. Karapetyan, A.A. Bush, R.P. Sukiasyan, *Mater. Chem. Phys.* 84 (2004) 79.
- [13] J. Ramajothi, S. Dhanuskodi, *Spectrochim. Acta Part A*, 68 (2007) 1213.
- [14] T. Mallik, T. Kar, *Mater. Lett.* 61 (2007) 3826.
- [15] Z. H. Sun, G. H. Zhang, X. Q. Wang, X. F. Cheng, X. J. Liu, L. Zhu, Y. Fan, G. Yu, D. Xu *J. Cryst. Growth*, 310 (2008) 2842.
- [16] A Criado, M.J. Dianez, S.P.L. Garrido, I.M. Fernandes, M.E. Belsley, M. De Gomes, *Acta Crystallogr. C*, 56 (2000) 888.
- [17] J. Zaccaro, J.P. Salvestrini, A. Ibanez, P. Ney, M.D. Fontana *J. Opt. Soc. Am.* 17 (2000) 427.
- [18] P. Anbusrinivasan, G. Madhurambal, S.C. Mojumdar, *J. Ther. Anal. Calori.* 96 (2009) 111.
- [19] D.S Chemla, J. Zyss 1987 *Nonlinear optical properties of organic molecules and crystals* (New York: Academic Press) Vols I & II.
- [20] S. Yamaguchi, M. Goto, H. Takayanagi, H. Ogura, *Bull. Chem. Soc. Jpn.* 61 (1988) 1026.
- [21] P. Zaderenko, M.S. Gel, P. Lopez, P. Ballesteros, I. Fonseca, A. Albert, *Acta Crystallogr. B*, 53 (1997) 961.
- [22] M.A.F. Elmosallamy, *Anal. Sci.* 20 (2004) 285.
- [23] R.G. Pearson, *J. Am. Chem. Soc.* 85 (1963) 3533.
- [24] R.G. Pearson, *Inorg. Chem.* 27 (1988) 734

- [25] R.G. Parr, L.V. Szentpaly, S. Liu, J. Am. Chem. Soc. 121 (1999) 1922.
- [26] T. Koopmans, Physica, 1 (1934) 104.
- [27] G. Venkatesh, M. Govindaraju, C. Kamal, P. Vennila, S. Kaya, RSC Adv. 7 (2017) 1401.
- [28] P. Vennila, M. Govindaraju, G. Venkatesh, C. Kamal, J. Mol. Struct. 1111 (2016) 151.
- [29] G. Venkatesh, M. Govindaraju, P. Vennila, Indian. J. Chem. 55 (2016) 413.

Access this Article in Online	
	Website: <a href="http://www.ijarm.com">www.ijarm.com</a>
	Subject: Chemistry
Quick Response Code	
DOI: <a href="https://doi.org/10.22192/ijamr.2022.09.02.003">10.22192/ijamr.2022.09.02.003</a>	

How to cite this article:

S. Sasikala, P. Anbusrinivasan, T. Dhanabal, B. Raja. (2022). Synthesis, spectral, NLO and DFT studies on 6-methylbenzotriazolium picrate crystal. Int. J. Adv. Multidiscip. Res. 9(2): 35-47.  
DOI: <http://dx.doi.org/10.22192/ijamr.2022.09.02.003>